

# Quantum Hamiltonian Algorithms for Maximum Independent Sets

Xianjue Zhao(赵贤觉),<sup>1</sup> Peiyun Ge(葛培云),<sup>2</sup> Hongye Yu(余泓烨),<sup>3</sup>  
Li You(尤力),<sup>2,4,5</sup> Frank Wilczek,<sup>6,7,8,9</sup> and Biao Wu(吴彪)<sup>1,10,\*</sup>

<sup>1</sup>International Center for Quantum Materials, School of Physics, Peking University, Beijing 100871, China

<sup>2</sup>State Key Laboratory of Low Dimensional Quantum Physics,

Department of Physics, Tsinghua University, Beijing 100084, China

<sup>3</sup>Department of Physics and Astronomy, Stony Brook University, Stony Brook, NY 11794, USA

<sup>4</sup>Frontier Science Center for Quantum Information, Beijing, China

<sup>5</sup>Beijing Academy of Quantum Information Sciences, Beijing 100193, China

<sup>6</sup>Center for Theoretical Physics, MIT, Cambridge, Massachusetts 02139, USA

<sup>7</sup>T. D. Lee Institute and Wilczek Quantum Center,

Shanghai Jiao Tong University, Shanghai 200240, China

<sup>8</sup>Department of Physics, Stockholm University, Stockholm SE-106 91, Sweden

<sup>9</sup>Department of Physics, Arizona State University, Tempe, Arizona 85287, USA

<sup>10</sup>Wilczek Quantum Center, School of Physics and Astronomy,

Shanghai Jiao Tong University, Shanghai 200240, China

(Dated: April 30, 2024)

Two quantum Hamiltonian algorithms have been proposed to solve the maximum independent set problem: the PK algorithm, introduced in [Phys. Rev. A **101** (2020) 012318; Chin. Phys. Lett. **38**, (2021) 030304], and the HV algorithm, presented in [Science **376** (2022) 1209]. Here we demonstrate that the two algorithms are mathematically equivalent. Specifically, the Hamiltonian in the PK algorithm can be viewed as the HV Hamiltonian in the interaction picture. Although they are mathematically equivalent, their most straightforward physical implementations are different, and our numerical simulations suggest that the PK algorithm might can bring significant advantages.

In a recent experiment [1], researchers successfully implemented a quantum Hamiltonian algorithm using Rydberg atom arrays to solve the maximum independent set (MIS) problem for a graph. We will refer to this algorithm as the HV algorithm in the following discussion. The HV algorithm uses the following Hamiltonian

$$\hat{H}_L = \frac{\hbar}{2} \sum_{j=1}^n [\Omega(t) e^{i\varphi(t)} |0\rangle_j \langle 1|_j + \text{h.c.} - 2\Delta(t) \hat{n}_j] + \sum_{i<j} V_{ij} \hat{n}_i \hat{n}_j, \quad (1)$$

where  $|0\rangle_j$  represents that the atom at site  $j$  not in the excited Rydberg state, while  $|1\rangle_j$  represents that it is excited. For a graph with  $n$  vertices of single atoms, the operator  $\hat{n}_j = |1\rangle_j \langle 1|_j$  denotes the Rydberg state fraction operator for site  $j$ . The term  $V_{ij}$  describes the interaction strength between two excited Rydberg atoms situated at sites  $i$  and  $j$ . A repulsive interaction  $V_{ij}$  imposes an energy penalty on multi-atom configurations in which both  $i$  and  $j \neq i$  are excited. Such interactions correspond, in the graph problem, to the existence of a line connecting the sites.  $\Omega(t), \varphi(t), \Delta(t)$  are control functions whose implementation defines the algorithm. In general, the goal of MIS algorithms of the type discussed here is to evolve into configuration with many disconnected excited states. These correspond to low-energy states at late times, when  $\Omega \rightarrow 0$  and  $\Delta$  approaches a positive constant.

With the pseudo-spin operators  $\sigma_j^z = 2\hat{n}_j - 1$ ,  $\sigma_j^+ = |1\rangle_j \langle 0|_j$ , and  $\sigma_j^- = |0\rangle_j \langle 1|_j$  we can rewrite the Hamiltonian  $H_L$  (up to an irrelevant time-dependent c-number) as

$$\hat{H}_L = \hat{H}_1(t) + \hat{H}_2, \quad (2)$$

where

$$\begin{aligned} \hat{H}_1(t) = & \frac{\hbar}{2} \Omega(t) \cos \varphi(t) \sum_j \sigma_j^x + \frac{\hbar}{2} \Omega(t) \sin \varphi(t) \sum_j \sigma_j^y \\ & - \frac{\hbar}{2} \Delta(t) \sum_j \sigma_j^z, \end{aligned} \quad (3)$$

and

$$\hat{H}_2 = \sum_{i<j} \frac{V_{ij}}{4} (1 + \sigma_i^z)(1 + \sigma_j^z). \quad (4)$$

Here  $\hat{H}_L$  is partitioned into two parts:  $\hat{H}_1(t)$ , a single-spin Hamiltonian which depends on time, and  $\hat{H}_2$ , the interactions between spins which is time-independent.

In references [2, 3], a seemingly different Hamiltonian we will refer to as the PK algorithm with

$$\hat{H}_A(t) = U(t) \hat{H}_0 U^\dagger(t), \quad (5)$$

was proposed to find the MIS of a graph, where

$$\hat{H}_0 = \frac{V_0}{4} \sum_{\langle i,j \rangle} (1 + \sigma_i^z)(1 + \sigma_j^z) = V_0 \sum_{\langle i,j \rangle} \hat{n}_i \hat{n}_j, \quad (6)$$

\* wubiao@pku.edu.cn

and  $U(t) = V(t)^{\otimes n}$  with  $V(t)$  being a unitary matrix for spin-1/2. When  $V(t)$  changes adiabatically as specified in the references, one can find the MIS as the ground state or its approximation, according to the PK algorithm.

We will demonstrate in the following that the Hamiltonians  $\hat{H}_L$  and  $\hat{H}_a$  are theoretically equivalent. The starting point is to note that  $\hat{H}_0$  and  $\hat{H}_2$  are essentially the same for  $V_{ij} > 0$ , or repulsive interaction between Rydberg atoms. This is because one can always choose a  $V_0 > 0$  such that all  $V_{ij} > V_0$ . In this case,  $\hat{H}_0$  and  $\hat{H}_2$  have the same set of ground states, which correspond to all independent sets of a given graph. Therefore, only  $\hat{H}_2$  will be referenced to in the following discussion.

## I. FROM SCHRÖDINGER PICTURE TO INTERACTION PICTURE

Consider a Hamiltonian system  $\hat{H}_S(t) = \hat{H}_1(t) + \hat{H}_2$ , which is similar to  $\hat{H}_L$ . The evolution of its wave function  $|\Phi_S(t)\rangle$  is described by the Schrödinger equation

$$i \frac{d}{dt} |\Phi_S(t)\rangle = [\hat{H}_1(t) + \hat{H}_2] |\Phi_S(t)\rangle. \quad (7)$$

We can go to the interaction picture with the following unitary evolution operator

$$U_I(t) = e^{-i \int_0^t \hat{H}_1(t') dt'}, \quad (8)$$

and the quantum state  $|\Phi_I(t)\rangle$  in the interaction picture is related to the state in the Schrödinger picture as follows

$$|\Phi_I(t)\rangle = U_I^\dagger(t) |\Phi_S(t)\rangle, \quad (9)$$

which satisfies the following equation

$$i \frac{d}{dt} |\Phi_I(t)\rangle = U_I^\dagger(t) \hat{H}_2 U_I(t) |\Phi_I(t)\rangle. \quad (10)$$

When  $U_I(t) = U^\dagger(t)$ , it is clear that the state  $|\Phi_I(t)\rangle$  will follow the evolution governed by the Hamiltonian  $\hat{H}_a(t)$  as specified in Eq. (5). With the form of  $U(t)$  given in Refs. [2, 3], the condition  $U_I(t) = U^\dagger(t)$  allows us to deduce  $\hat{H}_1(t)$ . If  $\hat{H}_1(t)$  takes the form of  $\hat{H}_1(t)$  in Eq. (3), the Hamiltonian  $\hat{H}_a(t)$  is equivalent to  $\hat{H}_L(t)$ .

In Refs. [2, 3],  $U(t) = V(t)^{\otimes n}$ , i.e., the tensor product of  $n$  identical single bit unitary matrix  $V(t)$  for

$$V(t) = \vec{n}(t) \cdot \vec{\sigma}, \quad (11)$$

where

$$\vec{n}(t) = (\sin \frac{\theta}{2} \cos \phi, \sin \frac{\theta}{2} \sin \phi, \cos \frac{\theta}{2}), \quad (12)$$

with  $\theta$  and  $\phi$  changing with time according to  $\theta = \omega_\theta t$ ,  $\phi = \omega_\phi t$ . In the simplest case when there is only one pseudo-spin in the system, we find  $U^\dagger(t) = V^\dagger(t) = \vec{n}(t) \cdot$

$\vec{\sigma}$ . Taking derivative with respect to time on both sides of  $U_I(t) = U^\dagger(t)$ , we obtain

$$\begin{aligned} -i \hat{H}_1 U_I(t) &= \vec{n}'(t) \cdot \vec{\sigma}, \\ \hat{H}_1 &= i(\vec{n}'(t) \cdot \vec{\sigma}) U_I^{-1}(t) = i(\vec{n}'(t) \cdot \vec{\sigma}) U(t), \\ &= i(\vec{n}'(t) \cdot \vec{\sigma})(\vec{n}(t) \cdot \vec{\sigma}), \\ &= i[(\vec{n}' \cdot \vec{n})I + i(\vec{n}' \times \vec{n}) \cdot \vec{\sigma}]. \end{aligned} \quad (13)$$

In the above  $\vec{n}'(t) = d\vec{n}(t)/dt$ . Since  $\vec{n}$  is a unit vector,  $\vec{n}'$  and  $\vec{n}$  are orthogonal to each other. As a result, we have

$$\hat{H}_1 = (\vec{n} \times \vec{n}') \cdot \vec{\sigma}. \quad (14)$$

Using  $\vec{n}(t) = (\sin \frac{\theta}{2} \cos \phi, \sin \frac{\theta}{2} \sin \phi, \cos \frac{\theta}{2})$ , we find

$$\begin{aligned} \vec{n}'(t) &= \omega_\phi (-\sin \frac{\theta}{2} \sin \phi, \sin \frac{\theta}{2} \cos \phi, 0) + \\ &\frac{1}{2} \omega_\theta (\cos \frac{\theta}{2} \cos \phi, \cos \frac{\theta}{2} \sin \phi, -\sin \frac{\theta}{2}). \end{aligned} \quad (15)$$

With  $\hat{H}_1 = (\vec{n} \times \vec{n}') \cdot \vec{\sigma}$ , we finally obtain

$$\begin{aligned} \hat{H}_1 &= -\omega_\phi \sin \frac{\theta}{2} (\cos \frac{\theta}{2} \cos \phi, \cos \frac{\theta}{2} \sin \phi, -\sin \frac{\theta}{2}) \cdot \vec{\sigma} \\ &- \frac{1}{2} \omega_\theta (\sin \phi, -\cos \phi, 0) \cdot \vec{\sigma}. \end{aligned} \quad (16)$$

The above derivation is easily extended to the case of  $n$  pseudo-spins, for which we find

$$\begin{aligned} \hat{H}_1 &= \left\{ -\omega_\phi \sin \frac{\theta}{2} (\cos \frac{\theta}{2} \cos \phi, \cos \frac{\theta}{2} \sin \phi, -\sin \frac{\theta}{2}) \right. \\ &\left. - \frac{1}{2} \omega_\theta (\sin \phi, -\cos \phi, 0) \right\} \cdot \sum_j \vec{\sigma}_j, \end{aligned} \quad (17)$$

which is of the same form of  $\hat{H}_1(t)$  in Eq. (3). We thus have shown that the Hamiltonian  $\hat{H}_a(t)$  is equivalent to  $\hat{H}_L(t)$ .

In the experiment [1], the quantum state is in the Schrödinger picture, which as we show above is related to the state in the interaction picture according to Eq. (9). At the end of the adiabatic evolution  $t = T$  specified in Ref. [3], we have  $\theta = \pi$  and  $\phi = 0$ . This means that

$$U_I^\dagger(T) = U(T) = [\vec{n}(T) \cdot \vec{\sigma}]^{\otimes n} = [\sigma_x]^{\otimes n}. \quad (18)$$

Its action is to flip every qubit, for example,

$$|11100\rangle \rightarrow |00011\rangle. \quad (19)$$

For the PK algorithm as discussed in Ref. [3], one needs to flip all the spins to get the right answer for the MIS. So the two flips cancel out and we can adopt  $|\Phi_S(t)\rangle$  obtained in the experiment as the final result.

## II. COMPARISON AND DISCUSSION

While the PK algorithm [2, 3] and the HV algorithm [1] are formally equivalent, they are motivated in different ways and offer different perspectives. The HV algorithm can be readily implemented experimentally while the PK algorithm gives an intuitive insight how the algorithm is capable of finding MIS in an inherently quantum way. Combined we now have a quantum MIS algorithm that is easy to implement experimentally and has great potential advantages over its classical counterparts.

The Hamiltonian  $\hat{H}_2$  has many degenerate ground states, which correspond to all the independent sets of a graph, and the minimum gap between them and the excited states is  $V_0$ , the minimum interaction strength between Rydberg atoms. When the changing rates  $\omega_\phi$  and  $\omega_\theta$  are much smaller than  $V_0/\hbar$  in the PK algorithm, the system stays and evolves in the sub-Hilbert space of the degenerate ground states of  $\hat{H}_2$ . Its evolution in the sub-Hilbert space is governed by a non-abelian gauge matrix  $A$ , which has a minimum energy gap  $\delta$ . When  $\omega_\theta/\omega_\phi \ll \delta$ , at the end of evolution  $T = \pi/\omega_\theta$ , the system has significant amplitudes to be in states which are either MIS or its good approximations [3]. It is clear from this insight that, for the quantum algorithm to be effective, one requires:

$$V_0/\hbar \gg \omega_\phi \gg \omega_\theta/\delta. \quad (20)$$

The explanation and physical origin of the dimensionless energy gap  $\delta$  can be found in Refs.[2, 3].

The two changing rates  $\omega_\phi$  and  $\omega_\theta$  in the PK algorithm [2, 3] are related to the parameters  $\Delta$ ,  $\Omega$  and  $\varphi$  in the experimental protocol [1] as follows:

$$\Delta(t) = -2\omega_\phi \sin^2 \frac{\omega_\theta t}{2}, \quad (21)$$

$$\varphi(t) = \arctan \frac{-\omega_\phi \sin \omega_\theta t \sin \omega_\phi t + \omega_\theta \cos \omega_\phi t}{-\omega_\phi \sin \omega_\theta t \cos \omega_\phi t - \omega_\theta \sin \omega_\phi t}, \quad (22)$$

$$\Omega(t) = \sqrt{\omega_\phi^2 \sin^2(\omega_\theta t) + \omega_\theta^2}, \quad (23)$$

This adiabatic path can be simplified further with a single bit unitary matrix  $V_s(t) = V(t)U_s(t) = (\vec{n}(t) \cdot \vec{\sigma})U_s(t)$ , where

$$U_s = \begin{pmatrix} 1 & 0 \\ 0 & e^{i\phi(t)} \end{pmatrix}. \quad (24)$$

The simplified path is given by

$$\Delta(t) = \omega_\phi \cos(\omega_\theta t), \quad (25)$$

$$\varphi(t) = \arctan \frac{-\omega_\theta}{\omega_\phi \sin(\omega_\theta t)} + \pi, \quad (26)$$

$$\Omega(t) = \sqrt{\omega_\phi^2 \sin^2(\omega_\theta t) + \omega_\theta^2}. \quad (27)$$

This is shown in Fig.1 as dashed lines. Our analysis below finds that this path has various advantages over the ones discussed in Ref.[1].

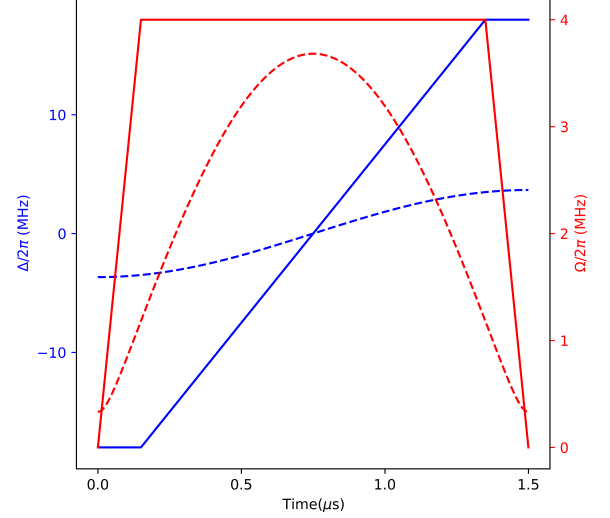


FIG. 1: The unoptimized path of VQAA is represented by the solid lines, same as the path given in FIG. S8. of [1]. The adiabatic path of the PK algorithm, given by Eqs. (25, 27), is drawn as the dashed lines with  $\omega_\theta = \pi/T$  and  $\omega_\phi/\omega_\theta = -11$ .

In Ref.[1], two different variational methods are used to find an optimized evolution path using classical mathematical search over a restricted set of trial paths. One is called the quantum approximate optimization algorithm (QAOA) and the other is called the variational quantum adiabatic algorithm (VQAA). For QAOA, it appears that the experimental protocol (as described above) does not quite implement the optimized evolution path faithfully, since that would require intermittent absence of interaction terms. For VQAA, it starts with an unoptimized path as shown Fig.1A and then the path is optimized with the help of a classical computer and experimental inputs.

We have compared the performances of the two paths in Fig.1 with graphs of seven vertices numerically. With 1000 graphs that are randomly generated, the PK algorithm has a minimum success rate of 83.784% and an average success rate of 97.370%. In contrast, the VQAA has an average success rate of 45.129%. Further numerical results show that in most cases where VQAA fail, the algorithms ends in states of non-independent sets, as shown in Fig.2C. Note that we set  $\varphi(t) = 0$  in our numerical computation. To implement PK algorithm faithfully, one actually needs to change  $\varphi(t)$  as Eq. (26). Numerical results show that this does not affect the performance of the PK algorithm. We find that with  $\varphi(t)$  changing as Eq. (26), the PK algorithm has a minimum success rate of 86.247% and an average success rate of 99.122%.

Optimized VQAA paths might be more competitive, but the excellent performance of a bare-bones implementation of PK is noteworthy.

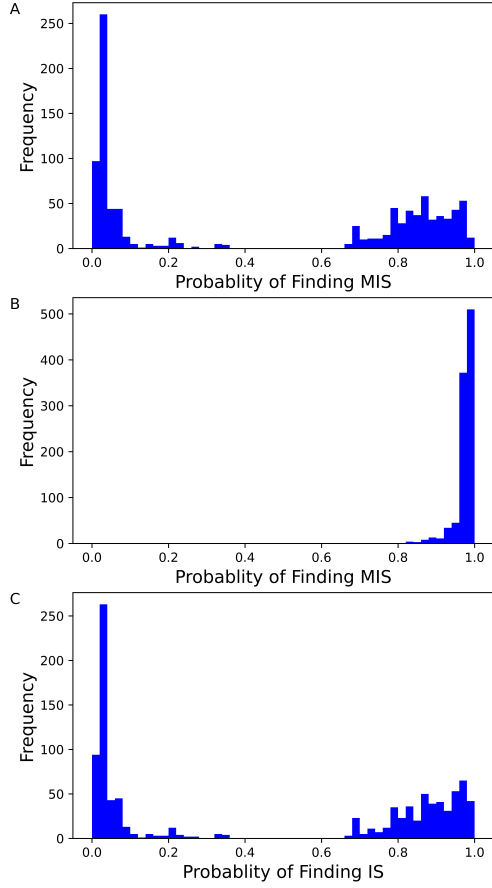


FIG. 2: **Performances of the VQAA and the PK algorithms on 1000 unit disk graphs with 7 vertices.** In the numerical simulation, we use parameters from the experiment [1], that is,  $V_{NN}/h = 107$  MHz,  $V_{NNN}/h = 13$  MHz,  $T = 1.5 \mu s$ . **(A).** The average success rate using the unoptimized path of VQAA is 45.129%. **(B).** The average success rate using the adiabatic path of the PK algorithm is 97.370%. **(C).** The average rate of ending in states of independent sets using the unoptimized path of VQAA is 46.132%, which means in most unsuccessful cases, the unoptimized path of VQAA leads to states of non-independent sets.

## ACKNOWLEDGMENTS

XJZ acknowledges discussions with Fangcheng Wang. XJZ and BW are supported by National Natural Science Foundation of China (Grants No. 92365202 and No. 11921005), and Shanghai Municipal Science and Technology Major Project (Grant No.2019SHZDZX01). PYG and LY are supported by the National Natural Science Foundation of China (NSFC)(Grants No. 12361131576 and No. 92265205), and by the Innovation Program for Quantum Science and Technology (2021ZD0302100). FW is supported by the U.S. Department of Energy under grant Contract Number DE-SC0012567, by the European Research Council under grant 742104, and by the Swedish Research Council under Contract No. 335-2014-7424.

---

[1] S. Ebadi, A. Keesling, M. Cain, T. T. Wang, H. Levine, D. Bluvstein, G. Semeghini, A. Omran, J.-G. Liu, R. Samajdar, X.-Z. Luo, B. Nash, X. Gao, B. Barak, E. Farhi, S. Sachdev, N. Gemelke, L. Zhou, S. Choi, H. Pichler, S.-T. Wang, M. Greiner, V. Vuletić, and M. D. Lukin, “*Quantum optimization of maximum independent set using Rydberg*

*atom arrays*”, Science **376**, 1209 (2022).  
 [2] Biao Wu, Hongye Yu, Frank Wilczek, “*Quantum independent-set problem and non-Abelian adiabatic mixing*”, Physical Review A **101**, 012318 (2020).  
 [3] Hongye Yu, Frank Wilczek, Biao Wu, “*Quantum Algorithm for Approximating Maximum Independent Sets*”, Chinese Physics Letters **38**, 030304 (2021).